Physica A 390 (2011) 4184–4191

Contents lists available at SciVerse ScienceDirect

Physica A

journal homepage: www.elsevier.com/locate/physa

The influence of nonmonotonic synchronized flow branch in a cellular automaton traffic flow model

Cheng-Jie Jin *, Wei Wang

School of Transportation, Southeast University of China, Nanjing, Jiangsu, 210096, People's Republic of China

ARTICLE INFO

Article history:
Received 26 May 2010
Received in revised form 18 June 2011
Available online 29 June 2011

Keywords:
Traffic flow
Cellular automaton
Synchronized flow
Congested patterns
Shock wave

ABSTRACT

In this paper we study the congested patterns upstream of an isolated on-ramp in a cellular automaton traffic flow model, which is proposed in our previous paper [Cheng-Jie Jin, Wei Wang, Rui Jiang, Kun Gao, J. Stat. Mech (2010) P03018]. The simulation results under open boundary conditions are presented by spatiotemporal diagrams. Our diagram of congested patterns is quite similar to that of the cellular automaton models within Kerner's three-phase traffic theory, while some differences in the "moving synchronized flow pattern" (MSP) should be noted. In our model the upstream front of MSP propagates not only upstream, but also downstream. The propagation direction depends on the flow rates and densities of free flow and synchronized flow. Besides, in our model the outflow of wide moving jams or bottlenecks could be free flow or synchronized flow, as reported in many empirical data. In the dissolving of congestions, the form of free flow may be hindered and stable synchronized flow may emerge. This phenomenon can help us understand more about the outflow. All the interesting characteristics of our model are due to the nonmonotonic structure of synchronized flow branch in the fundamental diagram, which has not been found in previous models.

1. Introduction

The systematic investigation of traffic flow has quite a long history [1–3]. Many models were carried out by various groups, in order to explain the empirical data. The earliest two approaches were the Lighthill–Whitham–Richards (LWR) kinematic wave traffic flow theory [4–6], and the general motors (GM) approach [7–9] based on car-following behaviors. In recent years, there are many new traffic flow models proposed from the viewpoint of statistical physics, especially at the mesoscopic and microscopic level: the optimal velocity (OV) model [10] and Davis's modified version [11], Tomer's model [12], the gas-kinetic-based traffic (GKT) model [13–15], the intelligent-driver model (IDM) [16,17], the variance-driven time headways (VDT) model [18], the Krauss's model [19–21], etc.

After the proposal of the famous Nagel–Schreckenberg (NS) model [22], the cellular automaton (CA) approach gradually attracted the interest of physicists, due to its fast and efficient performance in computer simulations. Then some CA models based on NS model were proposed, such as the VDR model [23,24], the VE model [25], the CD model [26,27], etc. In these models, traffic states were simply divided into two phases, the free flow phase (F) and the congested flow phase.

Based on the empirical data, Kerner thought the two-phase division is too rough to describe so many details of traffic flow. Thus, the interesting and important concept of "synchronized flow" was proposed, and congested flow is further classified into synchronized flow (S) and wide moving jams (J). The transitions among the three phases are of first-order. Usually before jams come to form, traffic flow turns from free flow to synchronized flow, and after that jams spontaneously emerge somewhere inside the synchronized flow region. The theory is called three-phase traffic theory [3,28].

* Corresponding author.
E-mail address: yitaikongtiao@gmail.com (C.-J. Jin).

0378-4371/$ – see front matter
doi:10.1016/j.physa.2011.06.057

There have been some models developed in Kerner's framework: the KKW model [29,30], the LEE model [31], the MCD model [32,33] and the VDE model [34,35]. The congested patterns upstream of an isolated on-ramp also have been studied in these papers. We have proposed a cellular automaton model in Ref. [36], in which the phase transition from synchronized flow to wide moving jams could be first-order without slow-to-start effect. Besides this, there are also some differences in the characteristics of synchronized flow branch in the fundamental diagram. In our model, the synchronized flow branch has two parts: the left one corresponding to light synchronized flow and the right one corresponding to heavy synchronized flow. It is non-monotonic, rather than monotonic in previous cellular automaton models. This feature is very interesting. It makes some influence on the isolated on-ramp traffic. In our simulation results, the moving synchronized flow pattern (MSP) is quite different from that of other three-phase traffic flow models. Its upstream front may propagate not only upstream, but also downstream. The propagation direction of this shock wave depends on the flow rates and densities of free flow (upstream) and synchronized flow (downstream), which will be discussed later.

It should be noted that in our model the outflow of wide moving jams or bottlenecks could be free flow or synchronized flow, which is quite different from previous models. Many empirical data [37–40] show that outflow is sometimes free flow and sometimes synchronized flow, but nearly no model can reproduce this phenomenon. In this paper we will give an intensive discussion for it.

This paper is organized as follows. In Section 2, we describe our model. In Section 3, we present our simulation results under open boundary conditions, not only the diagram of congested patterns, but also some supplement for the MSP and the outflow. Our conclusions are given in Section 4.

2. Model rules

For the sake of the completeness, we briefly recall our model proposed in Ref. [36]. We designed the velocity-updating rule with *anticipated deceleration* (AD) in the model, with which drivers prefer to decelerate when necessary. The anticipated safe velocity $V_{anti}(AD, gap)$ is the maximum of v satisfying the inequality:

$$B(v, AD) \leq gap.$$

Here $B(v, AD)$ is the whole distance that a vehicle travels before stopping if it keeps decelerating with AD from an initial velocity v. In cellular automaton models, function $B(v, AD)$ is often discredited. Suppose $m = \mathrm{int}(v/|AD|)$, then $B(v, AD)$ can be calculated as

$$\begin{aligned} B(v, AD) &= v + (v + AD) + (v + 2AD) + \cdots + (v + mAD) \\ &= (2v + mAD)(m + 1)/2. \end{aligned}$$

With the anticipated safe velocity $V_{anti}(AD, gap)$ calculated above, the model rules are executed on all vehicles in parallel as follows:

(1) Estimating the virtual velocity of the front vehicle (vehicle $n - 1$) [25]:

$$v'_{n-1} \to \min\{v_{\max} - 1, \max\{0, V_{anti}(AD, gap_{n-1}) - 1\}, v_{n-1}\};$$

(2) Deterministic acceleration or deceleration:

$$v_n \to \begin{cases} \min\{v_n + 1, v_{\max}\} & \text{when } v_n < gap_n + v'_{n-1} \text{ (Acceleration)} \\ V_{anti}(AD, gap_n + v'_{n-1}) & \text{when } v_n \geq gap_n + v'_{n-1} \text{ (Deceleration)} \end{cases}; \tag{1}$$

(3) Randomization:

$$v_n \to \max\{v_n - 1, 0\} \quad \text{with probability p;}$$

(4) Updating positions:

$$x_n(t + 1) \to x_n + v_n;$$

In the formulations above, $x_n(t)$ and $v_n(t)$ are the position and velocity of vehicle n at time t; vehicle $n - 1$ precedes vehicle n; gap_n is the distance between vehicle n and vehicle $n - 1$; and $v_{\max}$ is the speed-limitation of the vehicles.

It should be noted that AD is only an anticipated deceleration rather than a deceleration limitation as in Ref. [31]. If the deceleration has to be larger than $|AD|$ (especially in emergencies), it will be allowed in our model. Therefore vehicle collisions can be totally avoided.

Besides, we would like to mention that although the model rules presented here looks different from that in Ref. [36], they are actually the same because $V_{anti}(AD, gap) = v_n + A(gap, v_n, AD)$. Here $A(gap, v_n, AD)$ is the deceleration function defined in Ref. [36]. We believe the model rule in this paper is easier to understand.

3. Simulation results

In this section our simulation results are presented. Each cell is set to 1 m and each time step corresponds to 1 s. Each vehicle occupies 8 cells; the maximum velocity is set to 32 m/s, and the randomization parameters are set to $p = 0.01$. In this paper we set AD $= -8$ m/s^2.

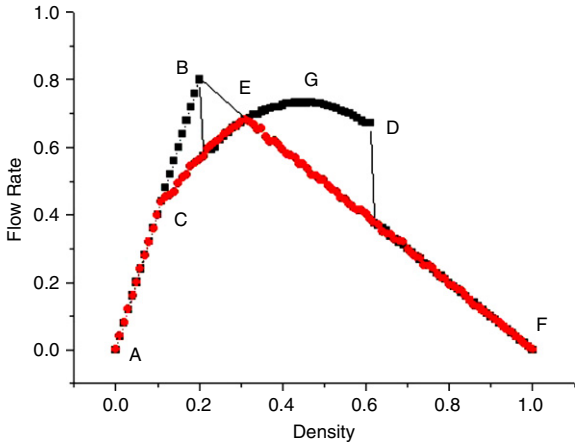

Fig. 1. (Color online) The fundamental diagram of our model. Here the black curve starts from homogeneous configuration and the red curve starts from megajam.

The fundamental diagram is shown in Fig. 1 for reference. Let us focus on the synchronized flow branch (Branch CD) of our model. It may be divided into two parts: the left part (Branch CG) with positive slope and the right part (Branch GD) with negative slope. It is non-monotonic, rather than monotonic in previous cellular automaton models. In the following simulations, we will see that there are two different types of synchronized flow: the light synchronized flow corresponding to the left branch (Branch CG), and the heavy synchronized flow corresponding to the right branch (Branch GD). They may be found in different spatiotemporal diagrams.

Since the simulations under periodic boundary conditions have been presented and discussed in Ref. [36], in this paper let us focus on the simulation features induced by an on-ramp under open boundary conditions, which are applied as follows: assuming the leftmost cell of the main road corresponds to $x = 1$ and the position of the leftmost vehicle is x_{last}, a new vehicle with velocity $V_{\max}$ will be inserted to the position with probability q_{in}, if $x_{last} > V_{\max}$. At the right boundary, the vehicles can move without any hindrance. When the position of the leading vehicle $x_{lead} > L$, in which L corresponds to the position of the exit, it will be removed and the second vehicle will become the leader.

At the on-ramp we adopt a simple configuration. In each time step, we scan the region $[x_{on}, x_{on} + L_{ramp}]$ to find out the largest gap. In order to let a vehicle come to the main road successfully, in real life this gap should be larger than the length of a vehicle. The minimum critical gap can be calculated by Kerner's method in Refs. [29,30]:

$$g^{(\min)} = \text{length} + \lambda^* v$$

where v is the velocity of the leading vehicle and λ is chosen to be equal to 0.2 in our simulations. If the gap is larger than the critical value, a new one will be inserted to the middle cells of it with probability q_{on}. The velocity of the newly inserted vehicle is set equal to the preceding vehicle. In this paper we set $x_{on} = 7000$ and $L_{ramp} = 100$. For all the spatiotemporal diagrams, we keep q_{in} constant during the simulation, and firstly set $q_{on} = 0$ for 10 000 time steps. Then the simulation time is set to 0, and the on-ramp injection q_{on} is turned on.

The diagram of congested patterns upstream of an isolated on-ramp can help us learn more about the characteristics of the CA model. Fig. 2 is the diagram which consists of six patterns: free flow (F), moving synchronized flow pattern (MSP), widening synchronized flow pattern (WSP), localized synchronized flow pattern (LSP), dissolving general pattern (DGP) and general pattern (GP). The boundaries between these patterns may vary with time, and in our simulations the diagram is drawn after 5000 time steps. The spatiotemporal diagrams of these congested patterns are shown in Fig. 3. With these parameters of flow rates, the evolution of patterns could be seen more clearly, especially for the first-order transitions between different traffic phases.

Generally speaking, our diagram of congested patterns is quite similar to that within Kerner's three-phase traffic theory. In Kerner's empirical data [37–40], different congested patterns upstream of an on-ramp are observed and discussed, including all the above six patterns. From comparison, we find the congested patterns simulated by our model could well coincide with the empirical ones. Based on the same observations, our model can present another possible modeling explanation for them. By simulations under open boundary conditions, we also find something different from previous three-phase CA models, such as the evolution of MSP, and the outflow of jams and bottlenecks. These interesting characteristics can help us learn more about the traffic flow in real life.

Firstly, the appearance of GP is shown in Fig. 3(a). The synchronized flow fixed at the bottleneck and some wide moving jams propagating upstream can be found. It is the most common congested pattern in empirical data. The downstream fronts of wide moving jams move with a constant velocity (about 15 km/h), which could be adjusted by the famous slow-to-start rule [23,24], as we discussed in Ref. [36]. In this figure we may find the outflow of wide moving jams and on-ramp bottlenecks are both synchronized flows, which is quite different from previous three-phase models [29–35]. In those

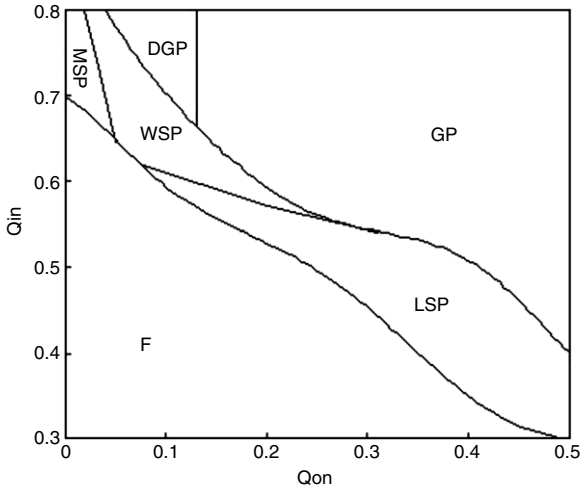

Fig. 2. The diagram of congested patterns induced by an isolated on-ramp when AD $= -8$ m/s^2. The simulation time $T = 5000$ s.

models the outflow is always free flow. Many empirical data [37–40] have shown that the outflow is sometimes free flow and sometimes synchronized flow, but nearly no model can reproduce this phenomenon. Later we will show how our model can do it.

When q_{on} is not so large, wide moving jams do not emerge, and only synchronized flows exist upstream of the bottleneck. This is the WSP within Kerner's framework. In Fig. 3(b) its downstream front is fixed at the bottleneck, while its upstream front is widening upstream.

When the value of q_{on} is between WSP and GP, another pattern called DGP occurs. In this pattern the transition from synchronized flow to jams occurs inside the WSP. However, it could not induce wide moving jams sequences, but only a jamming area dissolving over time, as Fig. 3(c) shows. Since the outflow of wide moving jams is synchronized flow, it is a little different from that in Kerner's model. The boundary between DGP and GP is a vertical line. Upon this boundary, the capacity of the on-ramp system equals the outflow rate of wide moving jams.

When q_{on} is large but q_{in} is not large enough, the upstream front of the synchronized flow cannot widen continuously. It is limited somewhere upstream of the on-ramp. This is the LSP within Kerner's framework, which can be seen in Fig. 3(d).

When q_{in} is quite large but q_{on} is very small, the MSP will occur. Even only one vehicle from the on-ramp can induce the $F \rightarrow S$ phase transition. In Fig. 3(e), synchronized flow propagating upstream and/or downstream could be observed. It firstly propagates upstream for a short distance, and then downstream for a longer distance. An enlarged figure of part of Fig. 3(e) is shown in Fig. 4(a). This type of synchronized flow has been presented by the spatiotemporal diagrams under periodic boundary conditions in our previous paper [36]. In Fig. 4(b) this situation is shown more clearly: the synchronized flow also changes its propagation direction during the $F \rightarrow S$ phase transition. It actually results from the decrease of upstream inflow.

The MSP in our model is quite different from that in other three-phase traffic flow models. We think the reason is due to the structure of the fundamental diagram. According to the famous shock wave theory, the propagating velocity of the upstream front of synchronized flow wave could be calculated by:

$$V = \frac{Q_u - Q_d}{\rho_u - \rho_d}$$

where Q_u/Q_d is the flow rate at upstream/downstream locations, and ρ_u/ρ_d is the density at upstream/downstream locations. Generally speaking, the density of synchronized flow is always higher than that of free flow, i.e. $\rho_u > \rho_d$. So when $Q_u > Q_d$, $V > 0$ and the upstream front propagates downstream, when $Q_u < Q_d$, $V < 0$ and it propagates upstream. Specially if $Q_u = Q_d$, $V = 0$ and the front can even keep constant. Since in our model the flow rates of synchronized flow may be higher than/lower than/equal to that of free flow, all the above three situations may occur. While in previous models, the flow rates of synchronized flow are always lower than that of free flow, so the MSP always propagates upstream.

In order to show the propagation of MSP more clearly, we will set the position of on-ramp nearer to the entrance of main road. Since the spontaneous $F \rightarrow S$ phase transition without bottlenecks may easily occur when the flow rate of the main road is very high, we could only maintain the stability of free flow with high rates in a short distance. When $x_{on} = 1000$, as shown in Fig. 4(c) & (d), a single vehicle from on-ramp may induce different propagation directions of MSP. By the comparison with the red vertical line, we may find the MSP propagates downstream when flow rate of free flow is 0.72, while it propagates upstream when the flow rate is 0.73. This interesting feature could not be found in previous models.

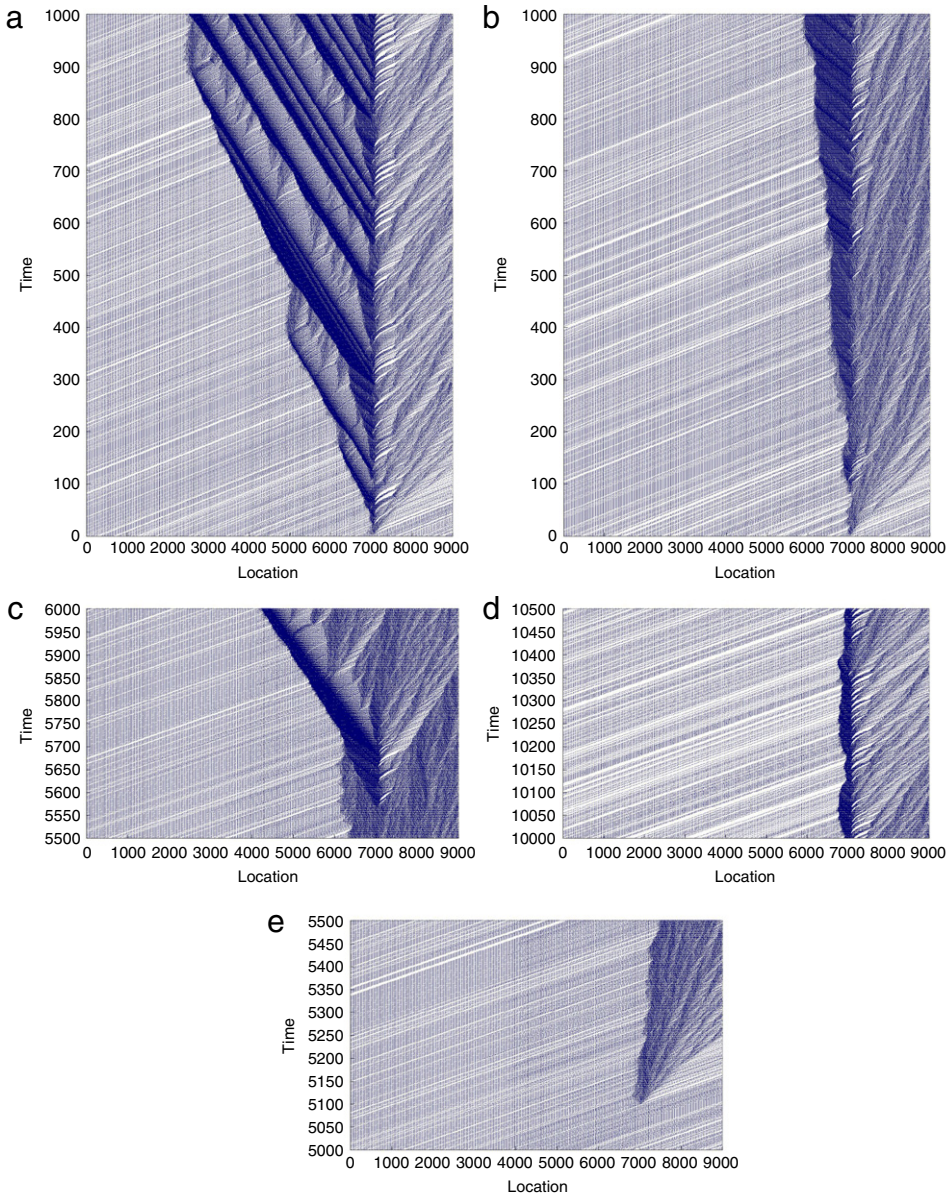

Fig. 3. The spatiotemporal diagrams of the congested patterns. (a) GP ($q_{in} = 0.7,\ q_{on} = 0.25$); (b) WSP ($q_{in} = 0.7,\ q_{on} = 0.1$); (c) DGP ($q_{in} = 0.71,\ q_{on} = 0.11$); (d) LSP ($q_{in} = 0.5,\ q_{on} = 0.4$); (e) MSP ($q_{in} = 0.7,\ q_{on} = 0.01$).

The characteristics of outflow in our model should also be noted. For most three-phase traffic flow models, in the fundamental diagram the curve starting from a megajam initial state only has two branches: free flow and wide moving jams. However, in our model it has three branches: not only free flow (Branch AC) and wide moving jams (Branch EF), but also synchronized flow (Branch CE). As Kerner pointed out in Refs. [38,40], in most three-phase traffic flow models, when free flow is formed in the outflow, the state is related to the point $(\rho_{\min}, q_{out})$ lying on the line J, and when synchronized flow is formed, the state is related to the point $(\rho_{\min}^{(syn)}, q_{out}^{(syn)})$ in the vicinity of the line J. But unfortunately in these models [29–35], the outflow of wide moving jams or bottlenecks is always free flow. The synchronized flow formed in the outflow cannot be simulated well, and the state "related to the point in the vicinity of the line J" cannot be found.

On the contrary, in our model the both types of outflow could be presented. When the outflow is synchronized flow, the state is related to the point E in Fig. 1. When it is free flow (i.e., the $F \rightarrow S$ phase transition does not occur), the state is related to point B, which is the intersection of the line J and the line of free flow. The free flow of Branch BC is metastable, while the synchronized flow of Branch CE is quite stable.

Our viewpoints above could be confirmed by some other simulation results. We set a virtual detector at the location of $X = 4000$ m (3000 m upstream of the bottleneck), and record the velocities of vehicles. When the flow rates are (0.7, 0.25),

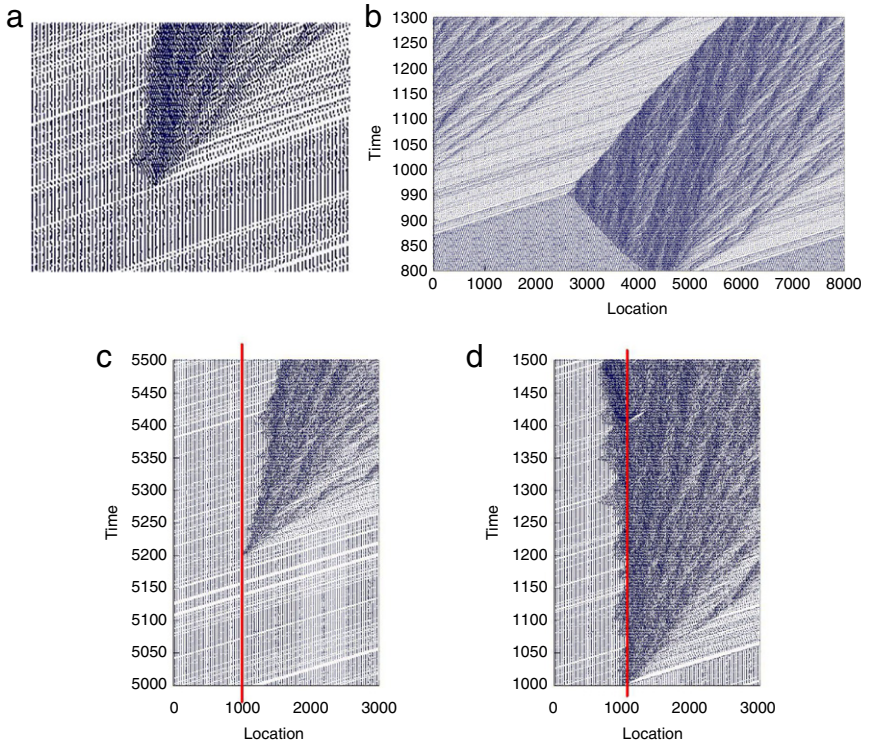

Fig. 4. Some typical spatiotemporal diagrams of different MSPs: (a) An enlarged figure of a part of Fig. 3(e); (b) MSP under periodic boundary conditions when $\rho = 0.3$; (c) MSP (0.72, 0.01) when $x_{on} = 1000$; (d) MSP (0.73, 0.01) when $x_{on} = 1000$.

as shown in Fig. 3(a), many wide moving jams can emerge upstream of the bottleneck. The snapshot of 230 vehicles is shown in Fig. 5(a). It is clear that the outflow of "Jam a" is free flow, since the recovery of traffic is not hindered; while the outflow of "Jam b" is synchronized flow, since traffic flow loses stability during the recovery. The reason why it loses stability is also due to spontaneous fluctuations. Fig. 5(b) is an enlarged figure of part of Fig. 3(a), in which different types of the outflow could be observed. The region surrounded by a black rectangle is covered by free flow, while the region surrounded by a red one is covered by synchronized flow. Therefore, it is easy to understand why in empirical data [37–40] the outflow is sometimes free flow and sometimes synchronized flow.

After the above simulations, we may find the new characteristics of our model are all due to the nonmonotonic structure of synchronized flow branch in the fundamental diagram. When the velocity of synchronized flow is high and the density is low, the synchronized flow may be considered as light. It corresponds to the left branch, as can be seen in the outflow of wide moving jams in GP and DGP, and in the outflow of bottlenecks in all the congested patterns. When the velocity is low and the density is high, the synchronized flow may be considered as heavy. It corresponds to the right branch, as can be seen in the synchronized flow fixed at the on-ramp in WSP and LSP. In our model MSP is a special case: it may correspond to either of the two branches according to different flow rates and densities. In previous three-phase CA models [29–35], the left branch of synchronized flow could not be found, so the outflow of wide moving jams and bottlenecks is always free flow, and the MSP always propagates upstream. This is the reason.

4. Conclusion

In this paper, we studied the congested patterns at an isolated on-ramp using a cellular automaton model proposed in our previous paper. Six different regions are presented and discussed: free flow, LSP, WSP, MSP, DGP and GP. The diagram of congested patterns is similar to many models based on Kerner's three-phase traffic theory, while our MSP has some different characteristics. In our model the MSP propagates not only upstream, but also downstream. The propagation direction depends on the flow rates and densities of free flow and synchronized flow. By the simulation results we can explain why in many empirical data the outflow is sometimes free flow and sometimes synchronized flow. This also helps to indicate the significance of our model. In a word, all the interesting characteristics of our model are due to the nonmonotonic structure of synchronized flow branch in the fundamental diagram.

Besides, since the propagation of the $F \rightarrow S$ phase transition without bottlenecks is difficult to be caught in real life, we think more empirical data is needed to check out this feature.

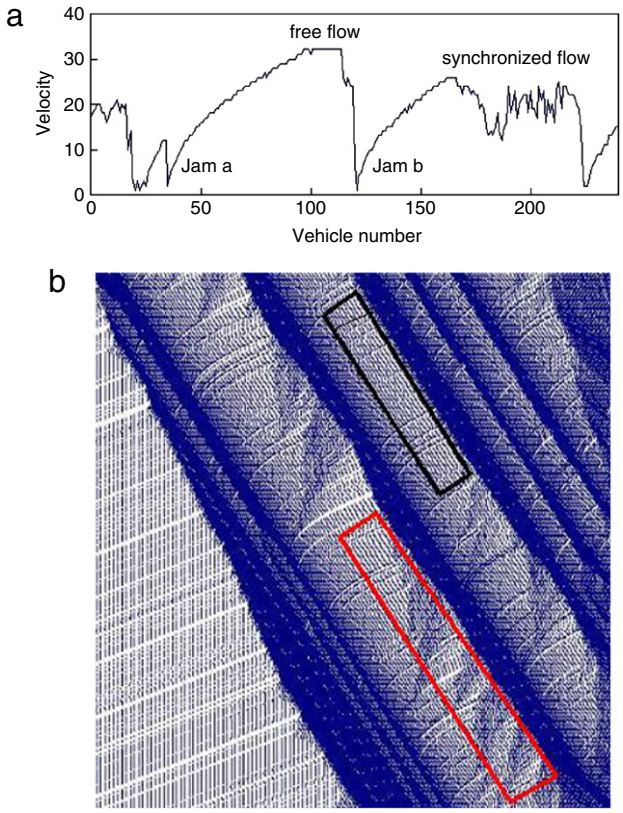

Fig. 5. Illustrations for the explanation of different types of the outflow of wide moving jams when flow rates are ($q_{in} = 0.7,\ q_{on} = 0.25$). (a) The velocity snapshot of 230 vehicles at $X = 4000$ m. (b) An enlarged figure of a part of Fig. 3(a).

Acknowledgments

The authors are very grateful to all the anonymous referees for valuable comments. We also thank Rui Jiang and Kun Gao for fruitful discussions. This work was funded by the National Natural Science Foundation of China (Grant No. 50738001).

References

[1] D. Helbing, Rev. Modern Phys. 73 (2001) 1067.
[2] D. Chowdhury, L. Santen, Andreas Schadschneider, Phys. Rep. 329 (2000) 199–329.
[3] B.S. Kerner, The Physics of Traffic, Springer, Berlin, 2004.
[4] M.J. Lighthill, G.B. Whitham, Proc. R. Soc. A 229 (1959) 281–345.
[5] P.I. Richards, Oper. Res. 4 (1956) 42–51.
[6] G.B. Whitham, Linear and Nonlinear Waves, Wiley, New York, 1974.
[7] R. Herman, E.W. Montroll, R.B. Potts, R.W. Rothery, Oper. Res. 7 (1959) 86–106.
[8] D.C. Gazis, R. Herman, R.W. Rothery, Oper. Res. 9 (1961) 545–567.
[9] D.C. Gazis, Traffic Theory, Springer, Berlin, 2002.
[10] M. Bando, K. Hasebe, A. Nakayama, A. Shibata, Y. Sugiyama, Phys. Rev. E 51 (1995) 1035.
[11] L.C. Davis, Phys. Rev. E 69 (2004) 016108.
[12] E. Tomer, L. Safonov, S. Havlin, Phys. Rev. Lett. 84 (2000) 382–385.
[13] D. Helbing, M. Treiber, Phys. Rev. Lett. 81 (1998) 3042–3045.
[14] D. Helbing, A. Hennecke, M. Treiber, Phys. Rev. Lett. 82 (1999) 4360–4363.
[15] M. Schönhof, D. Helbing, Transportation Science, 41 (2) 135–166.
[16] M. Treiber, A. Hennecke, D. Helbing, Phys. Rev. E 62 (2000) 1805.
[17] M. Treiber, D. Helbing, Phys. Rev. E 68 (2003) 046119.
[18] M. Treiber, A. Kesting, D. Helbing, Phys. Rev. E 74 (2006) 016123.
[19] S. Krauss, P. Wagner, C. Gawron, Phys. Rev. E 54 (1996) 3707.
[20] S. Krauss, P. Wagner, C. Gawron, Phys. Rev. E 55 (1997) 5597.
[21] A. Namazi, N. Eissfeldt, P. Wagner, A. Schadschneider, Eur. Phys. J. B 30 (2002) 559–570.
[22] K. Nagel, M. Schreckenberg, J. Physique I 2 (1992) 2221.
[23] R. Barlovic, L. Santen, A. Schadschneider, M. Schreckenberg, Eur. Phys. J. B 5 (1998) 793–800.
[24] R. Barlovic, A. Schadschneider, M. Schreckenberg, Physica A 294 (2001) 525–538.
[25] X.B. Li, Q.S. Wu, R. Jiang, Phys. Rev. E 64 (2001) 066l28.
[26] W. Knospe, L. Santen, A. Schadschneider, M. Schreckenberg, J. Phys. A: Math. Gen. 33 (2000) L477–L485.
[27] W. Knospe, L. Santen, A. Schadschneider, M. Schreckenberg, Phys. Rev. E 65 (2001) 015101.
[28] B.S. Kerner, Physica A 333 (2004) 379–440.

[29] B.S. Kerner, S.L. Klenov, D.E. Wolf, J. Phys. A: Math. Gen. 35 (2002) 9971–10013.
[30] B.S. Kerner, S.L. Klenov, J. Phys. A: Math. Gen. 35 (2002) L31–L43.
[31] H.K. Lee, R. Barlovic, M. Schreckenberg, D. Kim, Phys. Rev. Lett. 92 (2004) 238702.
[32] R. Jiang, Q.S. Wu, J. Phys. A: Math. Gen. 36 (2003) 381–390.
[33] R. Jiang, Q.S. Wu, Eur. Phys. J. B 46 (2005) 581–584.
[34] Kun Gao, Rui Jiang, Shou-xin Hu, et al., Phys. Rev. E 76 (2007) 026105.
[35] Kun Gao, Rui Jiang, Bing-Hong Wang, Qing-Song Wu, Phyisca A 388 (2009) 3233–3243.
[36] Cheng-Jie Jin, Wei Wang, Rui Jiang, Kun Gao, J. Stat. Mech (2010) P03018.
[37] B.S. Kerner, e-print in http://arxiv.org/abs/cond-mat/0309018.
[38] B.S. Kerner, Phys. Rev. E 65 (2002) 046138.
[39] B.S. Kerner, H. Rehborn, Phys. Rev. Lett. 79 (1997) 4030.
[40] B.S. Kerner, Phys. Rev. Lett. 81 (1998) 3797.